Lower atmosphere studies

Antarctic automatic weather stations: 1995–1996

ROBERT E. HOLMES, CHARLES R. STEARNS, *and* GEORGE A. WEIDNER, *Space Science and Engineering Center, University of Wisconsin, Madison, Wisconsin 53706*

The National Science Foundation's Office of Polar Programs places automatic weather station (AWS) units in remote areas in Antarctica in support of meteorological research, applications, and operations (see figure). The basic AWS units measure air temperature, air pressure, wind speed, and wind direction. Some units measure relative humidity and the air temperature difference (delta-T) between 3 meters (m) and 0.5 m above the surface at the time of installation. The data are collected by the ARGOS Data Collection System onboard the National Oceanic and Atmospheric Administration series of polar-orbiting satellites. Holmes, Weidner, and Stearns (1995) and Stearns, Weidner, and Holmes (1994) describe the AWS activities during the two previous austral summers.

Location information for the AWS units in operation in 1996 is given in the table. The AWS units are located in arrays for meteorological experiments and at other sites for operational purposes. Any one AWS may contribute to several experiments, and all can contribute to operational purposes.

Some of the areas supported are the following:

- katabatic wind flow down Reeves Glacier, Byrd Glacier, Beardmore Glacier, and the slopes to the Adélie and Siple Coasts;
- mesoscale circulation and the sensible and latent heat fluxes on the Ross Ice Shelf;
- climatology of Byrd and Dome C stations;
- boundary-layer meteorology around the South Pole;
- Long-Term Ecological Research (LTER) along the Antarctic Peninsula;
- meteorological support for flight operations at McMurdo Station, Antarctica.

The 1995–1996 antarctic field season began on 2 November 1995 when G.A. Weidner and R.E. Holmes left Madison, Wisconsin, for McMurdo Station, Antarctica, arriving on 6 November 1995.

A Twin Otter flight was made to Sandra AWS site on 8 November. The unit was removed completely, and AWS 8923 was returned to McMurdo to be repaired and redeployed at another site.

A Twin Otter flight was made on 9 November to Gill AWS site, but the site could not be located, so the flight continued to Schwerdtfeger AWS site. One 1.5-m tower section was added, and AWS 8913 was removed and returned to McMurdo to be repaired.

On 14 November, a Twin Otter flight to Elaine site was made. The aerovane was replaced, two boxes of three gel-cell batteries were installed, and the lower delta-T sensor was raised.

Pegasus North AWS site was visited by snowmobile on 17 November 1995. Two boxes of three gel-cell batteries were installed.

On 18 November, a Naval Support Force Antarctica (NSFA) helicopter flight was made to Linda AWS site. A Bendix aerovane was installed, but the unit continued to malfunction. On 24 November, a second NSFA helicopter flight was made to Linda AWS site. AWS 8915 was removed and replaced with AWS 8909.

Willie Field AWS site was visited by truck on 27 November 1995. Two boxes of three gel-cell batteries were installed, and the station was raised by one 1.8-m tower section. The Ultrasonic Depth Gauge (UDG) data were downloaded from the CR-10 data logger, and the UDG sensor was raised to a height of 1.36 m.

On 16 December, Charles Stearns and Jonathan Thom left Madison, Wisconsin, for the U.S. Coast Guard (USCG) *Polar Star* in Hobart, Tasmania, arriving there on 18 December. The *Polar Star* left Hobart on 20 December.

On 25 December, a USCG helicopter flight was made to D-10, and AWS 21364 was installed. A second USCG helicopter flight was made to Sutton site, but it could not be located. A flight was then made to Port Martin site. A new guy cable was installed. Next, a flight was made to Cape Denison, and the unit was found in good working order.

A USCG helicopter flight was made to Cape Webb on 26 December, and the unit was repaired. A second flight was made to Penguin Point, and the unit was repaired.

On 28 December, Greig Thompson left Madison, Wisconsin, for McMurdo Station, arriving there on 4 January 1996. Stearns and Thom arrived at McMurdo on 6 January.

On 16 January, Stearns, Thompson, and Thom left McMurdo Station for Up Stream Bravo. On 17 January, a Twin Otter flight was made to Elizabeth site, and AWS 21356 was removed and replaced with new 21361 electronics. The aerovane and the antenna cable were replaced.

The 1996 antarctic automatic weather station site name, ARGOS identification number, latitude, longitude, altitude above sea level, site start date, and WMO number for the Global Telecommunications System. Sites with three digits after the decimal point in the latitude and longitude were located using the ARGOS positions for a 3-day period.

Site	ARGOS ID	Latitude (deg)	Longitude (deg)	Altitude (in meters)	Date start	WMO number
			Adélie Coast			
D-10	8919b[b]	66.71 °S	139.83 °E	243	Jan 80	89832
D-47	8986[b]	67.397°S	138.726°E	1,560	Nov 82	89834
D-57	21360[b]	68.199°S	137.538°E	2,105	Jan 96	
D-80	8916[b]	70.040°S	134.878°E	2,500	Jan 83	89836
Dome C II[a]	8989	75.121°S	123.374°E	3,250	Dec 95	89828
Port Martin	8930	66.82 °S	141.40 °E	39	Jan 90	
Cape Denison	8907	67.009°S	142.664°E	31	Jan 90	
Penguin Point	8929	67.617°S	146.180°E	30	Dec 93	89847
Sutton	8939	67.08 °S	141.37 °E	871	Dec 94	
Cape Webb	8933	67.934°S	146.824°E	37	Dec 94	
			West Antarctica			
Byrd Station	8903	80.007°S	119.404°W	1,530	Feb 80	89324
Brianna	21362	83.887°S	134.145°W	549	Nov 94	
Elizabeth	21361[b]	82.606°S	137.082°W	549	Nov 94	89332
J.C.	21357	85.070°S	135.516°W	549	Nov 94	
Erin	21363[b]	84.901°S	128.810°W	1,006	Nov 94	
Harry	21355	83.003°S	121.393°W	945	Nov 94	
Theresa	21358	84.599°S	115.811°W	1,463	Nov 94	89314
Doug	21359	82.315°S	113.240°W	1,433	Nov 94	
Mount Siple	8981	73.198°S	127.052°W	230	Feb 92	89327
			Ross Island region			
Marble Point	8906	77.439°S	163.759°E	120	Feb 80	89866
Ferrell	8934	77.928°S	170.820°E	45	Dec 80	89872
Pegasus North	8927	77.952°S	166.505°E	10	Jan 90	89667
Pegasus South	8937	77.990°S	166.576°E	10	Jan 91	
Minna Bluff	8988	78.554°S	166.656°E	920	Jan 91	89768
Linda	8909[b]	78.480°S	168.375°E	50	Jan 91	89769
Willie Field	8901	77.865°S	167.017°E	40	Jan 92	
			Ocean islands			
Whitlock	8921	76.144°S	168.392°E	274	Jan 82	89865
Scott Island	8983	67.37 °S	179.97 °W	30	Dec 87	89371
Young Island	8980	66.229°S	162.275°E	30	Jan 91	89660
Possession Island	8984	71.891°S	171.210°E	30	Dec 92	89879
			Ross Ice Shelf			
Marilyn	8931	79.954°S	165.130°E	75	Jan 84	89869
Schwerdtfeger	8913	79.904°S	169.973°E	60	Jan 85	89868
Gill	8911	79.985°S	178.611°W	55	Jan 85	89376
Elaine	8900	83.134°S	174.169°E	60	Jan 86	89873
Lettau	8908	82.518°S	174.452°W	55	Jan 86	89377
			Reeves Glacier			
Manuela	8905	74.946°S	163.687°E	80	Feb 84	89864
Lynn	8935	74.207°S	160.409°E	1,772	Jan 88	89860
			Antarctic Peninsula			
Larsen Ice	8926	66.949°S	60.914°W	17	Oct 85	89262
Butler Island	8902	72.207°S	60.171°W	91	Mar 86	89266
Uranus	8920	71.43 °S	68.93 °W	780	Mar 86	89264
Limbert[a]	8925	75.422°S	59.948°W	40	Dec 95	
Racer Rock	8947	64.067°S	61.613°W	17	Nov 89	89261
Bonaparte Point	8912	64.778°S	64.067°W	8	Jan 92	89269
AGO-A84[a]	8932	84.36 °S	23.86 °W	2,103	Jan 96	
Ski-Hi	8917	74.975°S	70.766°W	1,395	Feb 94	89272
Santa Claus I	8910	64.964°S	65.670°W	25	Dec 94	

Site	ARGOS ID	Latitude (deg)	Longitude (deg)	Altitude (in meters)	Date start	WMO number
			High polar plateau			
Clean Air	8987	90.00 °S		2,835	Jan 86	89208
Henry	8985	89.011°S	1.025°W	2,755	Jan 93	89108
Nico	8924	89.000°S	89.669°E	2,935	Jan 93	89799
Relay Station	8918	74.017°S	43.062°E	3,353	Feb 95	89744
Dome Fuji	8982	77.31 °S	39.70 °E	3,810	Feb 95	89734

[a]New locations for 1996.
[b]New ARGOS ID for 1996 at the site.

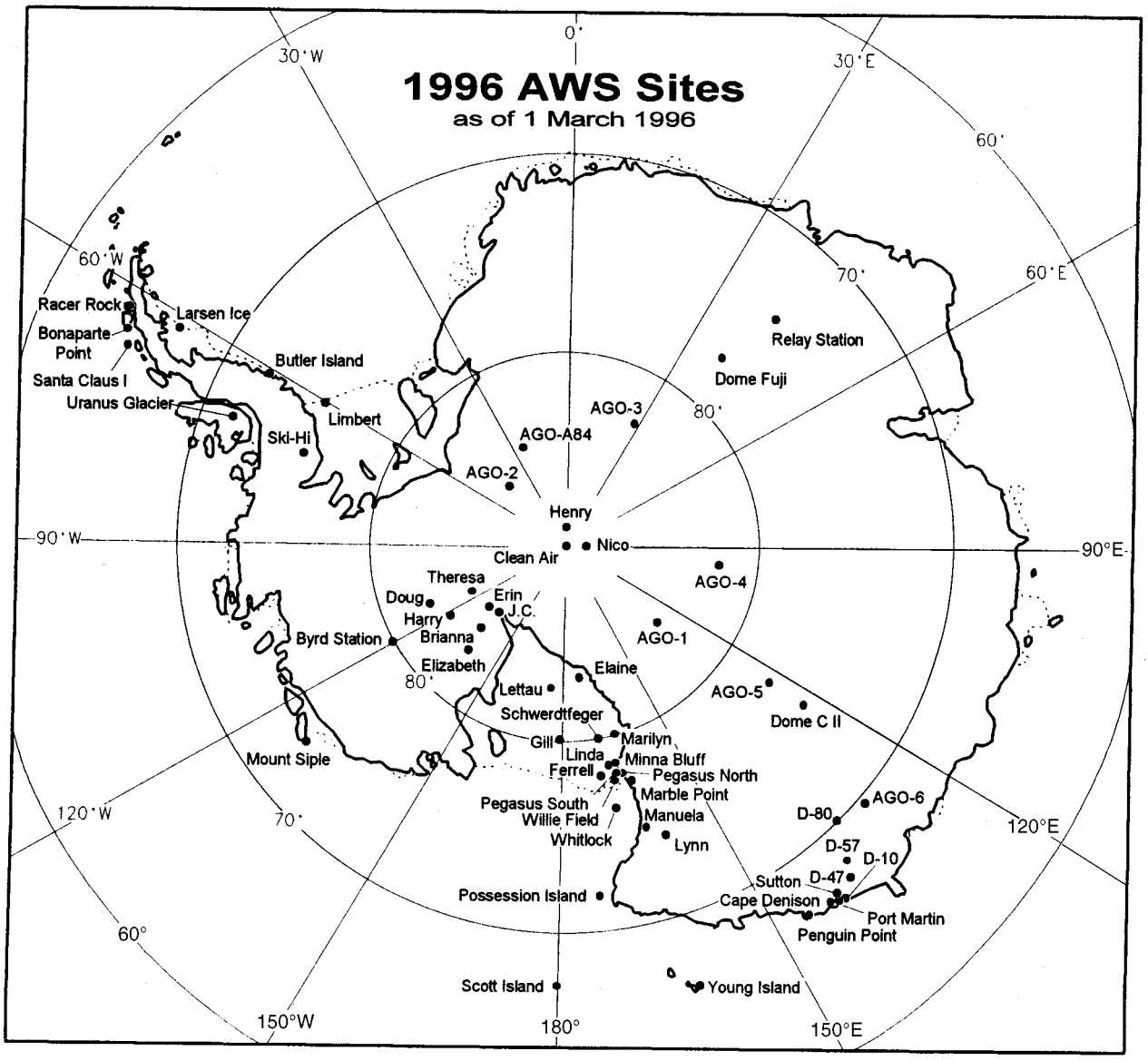

Map of Antarctica showing the locations of widely spaced automatic weather stations for 1996. The locations of the AGO sites are included but are not part of the AWS program.

On 18 January, a Twin Otter flight was made to J.C. site. The unit was repaired, but the malfunctioning wind direction was not investigated because of the high wind speed at the time of the site visit. The flight continued on to Erin site, where the antenna cable was replaced, but the unit still did not transmit. Because of limited resources, the electronics were not replaced at that time. A second Twin Otter flight was made to Theresa site, and the unit was repaired. A flight to Erin site was then made, and AWS 21361 was replaced with 21363. A Belfort aerovane was also installed.

On 19 January, Stearns, Thom, and Thompson returned to McMurdo Station by LC-130.

On 23 January, a Twin Otter flight was made to Marilyn site. The site was raised, and two boxes of three gel-cell batteries were installed. A new power junction box, antenna, and solar panel were also installed. The following day, a Twin Otter flight was made to Gill site and the site was raised.

A Twin Otter flight was made to Schwerdtfeger site on 27 January, and AWS 8913 was installed. A Bendix aerovane was installed as well as two boxes of three gel-cell batteries and new battery cables.

Crew members of the USCG *Polar Star* installed dog house AWS 8980 at Young Island. Dog house AWS 8983 was not installed at Scott Island because of fog.

On the Antarctic Peninsula, members of the British Antarctic Survey raised the AWS unit at Uranus Glacier on 28 November and installed AWS 8925 on the Ronne Ice Shelf on 30 November. On 10 December, Ski Hi site was visited; the station was in good working order and did not need to be raised. Members of the LTER group replaced the batteries at Bonaparte Point AWS site on 14 January and installed a sea-water temperature probe at Santa Claus Island AWS site on 13 February. The sea-water temperature probe did not function properly.

Members of Programma Nazionle di Ricerche in Antartide at Terra Nova Bay installed a Belfort aerovane at Manuela site. The aerovane was delivered to them by the *Polar Star* on the refueling trip for the base.

Members of Institut Français pour la Recherche et la Technologie Polaires (IFRTP) installed AWS 8989 at Dome-C II on 12 December. On 15 December, Dome-C site was disconnected from the Radioactive Thermonuclear Generator and was connected to batteries. The station ran for approximately 18 days before the batteries were drained of power, and the unit was removed. AWS 8914 was removed from D-80, and AWS 8916 was installed on 24 January. In early February, AWS 21360 was installed at D-57, and AWS 8986 was installed at D-47. Also, AWS 21364 was removed from D-10 on 21 January and replaced with AWS 8919.

We were assisted in Antarctica by Jonathan Thom and Greig Thompson of the Department of Atmospheric and Oceanic Sciences, University of Wisconsin, NSFA–Meteorology, and by the crews of the Twin Otters, LC-130s, NSFA helicopters, USCG helicopters, and the USCG *Polar Star*. The AWS program is supported by National Science Foundation grant OPP 94-19128.

References

Holmes, R.E., G.A. Weidner, and C.R. Stearns. 1995. Antarctic automatic weather stations: 1994–1995. *Antarctic Journal of the U.S.,* 30(5), 327–329.

Stearns, C.R., G.A. Weidner, and R.E. Holmes. 1994. Antarctic automatic weather stations: Austral summer 1993–1994. *Antarctic Journal of the U.S.,* 29(5), 281–284.

Antarctic automatic weather stations: 1996–1997

CHARLES R. STEARNS, ROBERT E. HOLMES, *and* GEORGE A. WEIDNER, *Space Science and Engineering Center, University of Wisconsin, Madison, Wisconsin 53706*

The National Science Foundation's Office of Polar Programs places automatic weather station (AWS) units in remote areas in Antarctica in support of meteorological research, applications, and operations (*see* figure). The basic AWS units measure air temperature, wind speed, and wind direction at a nominal height of 3 meters above the surface. Air pressure is measured at the height of the electronics enclosure. Some units measure relative humidity at 3 meters above the surface and the air temperature difference between 3 meters and 0.5 meters above the surface at the time of installation. The data are collected by the ARGOS Data Collection System onboard the National Oceanic and Atmospheric Administration series of polar-orbiting satellites.

The table gives the AWS unit's site name, ARGOS identification number, latitude, longitude, elevation above sea level, site start date, and World Meteorological Organization (WMO) number for the Global Telecommunications System for AWS units in operation in 1997. The AWS units are grouped together based on the geographical area and are usually related to a single meteorological experiment. Holmes,

The 1997 antarctic automatic weather station site name, ARGOS identification number, latitude, longitude, altitude above sea level, site start date, and WMO number for the Global Telecommunications System. Sites with three digits after the decimal point in the latitude and longitude were located using the ARGOS positions for a 3-day period, aircraft global positioning system (GPS), or hand-held GPS.

Site	ARGOS ID	Latitude (deg)	Longitude (deg)	Altitude (in meters)	Date start	WMO number
			Adélie Coast			
D-10	8919	66.71 °S	139.83 °E	243	Jan 80	89832
D-47	8986	67.397°S	138.726°E	1,560	Nov 82	89834
D-57	21360	68.199°S	137.538°E	2,105	Jan 96	
D-80	8916	70.040°S	134.878°E	2,500	Jan 83	89836
Dome C II	8989	75.121°S	123.374°E	3,250	Dec 95	89828
Port Martin	8930	66.82 °S	141.40 °E	39	Jan 90	
Cape Denison	8907	67.009°S	142.664°E	31	Jan 90	
Penguin Point	8929	67.617°S	146.180°E	30	Dec 93	89847
Sutton	8939	67.08 °S	141.37 °E	871	Dec 94	
Cape Webb	8933	67.934°S	146.824°E	37	Dec 94	
			West Antarctica			
Byrd Station	8903	80.007°S	119.404°W	1,530	Feb 80	89324
Brianna	21362	83.887°S	134.145°W	549	Nov 94	
Elizabeth	21361	82.606°S	137.082°W	549	Nov 94	89332
J.C.	21357	85.070°S	135.516°W	549	Nov 94	
Erin	21363	84.901°S	128.810°W	1,006	Nov 94	
Harry	21355	83.003°S	121.393°W	945	Nov 94	
Theresa	21358	84.599°S	115.811°W	1,463	Nov 94	89314
Doug	8922[a]	82.315°S	113.240°W	1,433	Nov 94	
Mount Siple	8981	73.198°S	127.052°W	230	Feb 92	89327
Siple Dome[b]	8900	81.656°S	148.773°W	620	Jan 97	89345
Swithinbank[b]	21356	81.200°S	126.174°W	945	Jan 97	
			Ross Island region			
Marble Point	8906	77.439°S	163.759°E	120	Feb 80	89866
Ferrell	8934	77.928°S	170.820°E	45	Dec 80	89872
Pegasus North	8927	77.952°S	166.505°E	10	Jan 90	89667
Pegasus South	8937	77.990°S	166.576°E	10	Jan 91	
Minna Bluff	8988	78.554°S	166.656°E	920	Jan 91	89768
Linda	8909	78.480°S	168.375°E	50	Jan 91	89769
Willie Field	8901	77.865°S	167.017°E	40	Jan 92	
			Ocean islands			
Whitlock	8921	76.144°S	168.392°E	274	Jan 82	89865
Scott Island	8983	67.37 °S	179.97 °W	30	Dec 87	89371
Young Island	8980	66.229°S	162.275°E	30	Jan 91	89660
Possession Island	8984	71.891°S	171.210°E	30	Dec 92	89879
			Ross Ice Shelf			
Marilyn	8931	79.954°S	165.130°E	75	Jan 84	89869
Schwerdtfeger	8913	79.904°S	169.973°E	60	Jan 85	89868
Gill	8911	79.985°S	178.611°W	55	Jan 85	89376
Elaine	8915[a]	83.134°S	174.169°E	60	Jan 86	89873
Lettau	8908	82.518°S	174.452°W	55	Jan 86	89377
			Reeves Glacier			
Manuela	8905	74.946°S	163.687°E	80	Feb 84	89864
Lynn	8935	74.207°S	160.409°E	1,772	Jan 88	89860
			Antarctic Peninsula			
Larsen Ice	8926	66.949°S	60.914°W	17	Oct 85	89262
Butler Island	8902	72.207°S	60.171°W	91	Mar 86	89266
Uranus	8920	71.43 °S	68.93 °W	780	Mar 86	89264
Limbert[a]	8925	75.422°S	59.948°W	40	Dec 95	
Racer Rock	8947	64.067°S	61.613°W	17	Nov 89	89261
Bonaparte Point	8923[a]	64.778°S	64.067°W	8	Jan 92	89269

Site	ARGOS ID	Latitude (deg)	Longitude (deg)	Altitude (in meters)	Date start	WMO number
AGO-A84[a]	8932	84.36 °S	23.86 °W	2,103	Jan 96	
Ski-Hi	8917	74.975°S	70.766°W	1,395	Feb 94	89272
Santa Claus I	21364[a]	64.964°S	65.670°W	25	Dec 94	
			High polar plateau			
Clean Air	8987	90.00 °S		2,835	Jan 86	89208
Henry	8985	89.011°S	1.025°W	2,755	Jan 93	89108
Nico	8924	89.000°S	89.669°E	2,935	Jan 93	89799
Relay Station	8918	74.017°S	43.062°E	3,353	Feb 95	89744
Dome Fuji	8904-8982[a]	77.31 °S	39.70 °E	3,810	Feb 95	89734

[a]New locations for 1997.
[b]New ARGOS ID for 1997 at the site.

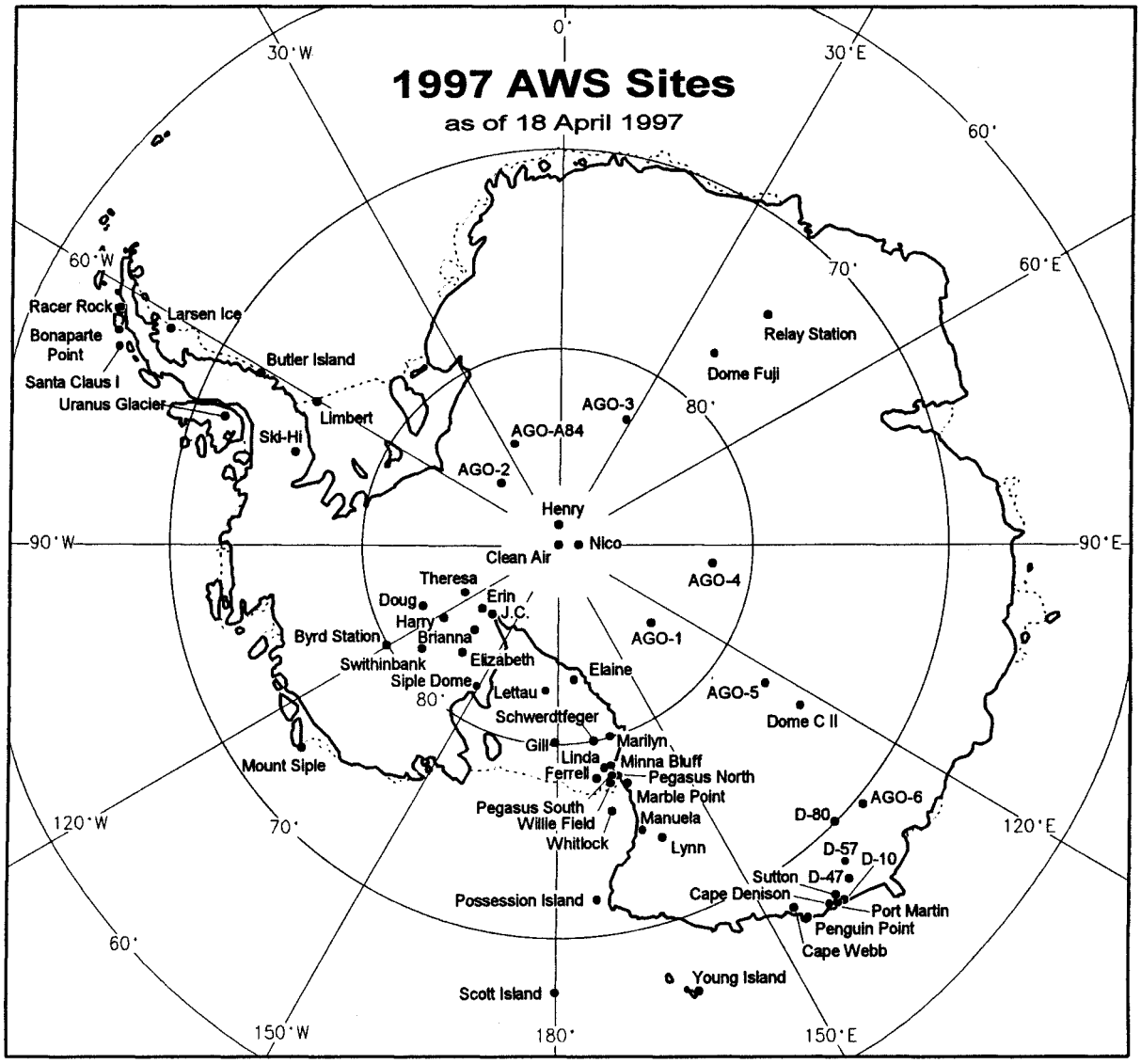

Map of Antarctica showing the locations of widely spaced automatic weather stations for 1997. Identification of the sites is by the site name. The locations of the AGO 1 to 6 sites are included but are not a part of the AWS program.

Weidner, and Stearns (1995) and Holmes, Weidner, and Stearns (1997) describe the AWS activities during the two previous field seasons.

The AWS units are located in arrays for meteorological experiments and at other sites for operational purposes. Any one AWS may contribute to several experiments and all contribute to operational purposes, especially for preparing weather forecasts for aircraft flights to and from New Zealand and within Antarctica.

Some of the areas supported are the following:

- barrier wind flow along the Antarctic Peninsula and the Transantarctic Mountains;
- katabatic wind flow down Reeves Glacier, Byrd Glacier, Beardmore Glacier, Siple Coast, and the slope to the Adélie Coast;
- mesoscale circulation and the sensible and latent heat fluxes on the Ross Ice Shelf;
- climatology of Byrd and Dome C stations;
- meteorological support around the South Pole;
- meteorological support for West Antarctic Ice Sheet Initiative and the International Trans-Antarctic Scientific Expedition;
- Long-Term Ecological Research (LTER) along the Antarctic Peninsula; and
- meteorological support for flight operations at McMurdo, Antarctica.

The AWS data are available via anonymous ftp on the Internet by contacting *ftp uwaaws.ssec.wisc.edu*. At "user" type "anonymous"; at "password," type your electronic mail address then "cd pub"—this puts you in the public directory where several "readme" files will guide you to what you want. The first file to read is *readme.faq*. If you have problems then e-mail *chucks@ssec.wisc.edu* or *front242@uwamrc.ssec.wisc.edu* requesting help. Additional meteorological data are on

- *uwamrc.ssec.wisc.edu*
- *http://uwamrc.ssec.wisc.edu/amrchome.html*
- *http://www.ssec.wisc.edu/~rbrbrn/awsproj.html*

The automatic weather station data are also available at 3-hour intervals on floppy disks starting in 1980. The yearly data books prior to 1994 contain 3-hourly data and monthly summaries. Starting in 1995, the yearly data book does not have the 3-hourly data.

Antarctic Peninsula

The 1996–1997 antarctic field season began with Tony Amos traveling aboard the *Polar Duke* to repair the AWS units on Bonaparte Point and Santa Claus Island. At Bonaparte Island, Tony Amos replaced the AWS electronics, batteries, and boom. The electronic box connectors to the boom and junction box were replaced with connectors that are supposed to be capable of withstanding corrosion by salt water. The connections between the junction box and the batteries and solar panel were wired directly and the openings were plugged up with modeling clay. The water temperature sensor was installed in the sea water at Bonaparte Point. At Santa Claus Island, the replacements were similar to those at Bonaparte Point. At Racer Rock, the AWS unit is operating intermittently, but the equipment was not available to make the necessary repairs.

The parts removed from the two sites were returned to the University of Wisconsin in March 1997. The condition of the boom and other parts such as the antenna indicates that several changes need to be made to make sure the AWS units withstand the corrosion of sea water. All sensors returned were not repairable.

The field season activities based out of McMurdo Station, Antarctica, began 21 December 1996 when R.E. Holmes left Madison, Wisconsin, for McMurdo Station, arriving on 26 December 1996.

On 2 January 1997, a Twin Otter flight was made to Elaine AWS site. The site was raised by one 0.9-meter (m) tower section and the lower delta-T sensor was raised to a height of 1.0 m. AWS 8900 was replaced with AWS 8915.

On 17 January, R.E. Holmes left McMurdo Station for Siple Dome field camp via LC-130. On 18 January, Byrd AWS site was visited by Twin Otter. The unit began operating after disconnecting and reconnecting power. The unit was raised by one 1.5-m tower section. The solar panels and power junction box were also replaced. Also on 18 January, a new AWS site was installed in West Antarctica via Twin Otter at a site named "Swithinbank" after Charles Swithinbank of the British Antarctic Survey because he was very helpful to C.R. Stearns at the beginning of the weather station program. AWS 21356 was installed.

On 20 January, a Twin Otter flight was made to J.C. AWS site. The aircraft was unable to land because of fog at J.C. site and continued on to Doug AWS site. AWS 21359 was removed and replaced with AWS 8922.

On 21 January, a new AWS site near the Siple Dome field camp was installed. AWS 8900 was installed approximately 3 kilometers to the true east of the field camp. Also on this day, the crew of the Twin Otter visited J.C. AWS site on their way to South Pole and replaced the R.M. Young wind sensor and installed two boxes of three gel-cell batteries.

The Coast Guard icebreaker crew under the direction of Lt. John Talbert replaced the wind system at Manuela site despite the –50°C wind chill. The crew installed a dog house AWS unit, ID 8983, on Scott Island and were able to remove the electronics, thermometer, and antenna from the old unit. This is the first time we have recovered components from a dog house AWS unit that has stopped operating. We now have the triangle of Young Island, Possession Island, and Scott Island operational again.

Adélie Coast

Members of Institut Française pour la Recherche et la Technologic Polaires removed the AWS units at D-10, D-47, D-57, and D-80 for repair and returned them to Madison, Wisconsin. The units are expected to be installed in December 1997 on a traverse to Dome C. AWS 8914 was shipped to Dumont D'Urville for installation at D-10 when the sea ice between Dumont d'Urville and the Adélie Coast is strong enough to permit travel between the two points.

British Antarctic Survey

The British Antarctic Survey (BAS) visited the Larsen Ice Shelf site. The tower was raised 0.9 m, two deadman and guys were installed, and the wind vane and prop were replaced. The site is 29 kilometers from the ice edge. Next season, the battery cables will need to be extended, and the tower will need to be raised again. At Butler Island site the tower was raised 0.9 m, and the wind vane was replaced. Next season, the tower will need raising again, and another deadman and rope will be needed along with battery extension cables for two battery boxes. At Uranus Glacier one 0.9-m tower section was added and new deadman and guys were installed.

WMO numbers have been assigned to Siple Dome AWS and Limbert AWS sites, and the data are entering the Global Telecommunications System (GTS).

Tony Amos did an excellent job of taking care of the AWS sites at Bonaparte Point and Santa Claus Island for LTER. We received assistance from Naval Support Force Antarctica (NSFA) Meteorology, and the crews of the Twin Otter aircraft, LC-130s, NSFA helicopters, the U.S. Coast Guard *Polar Star*, and U.S. Coast Guard helicopters. The British Antarctic Survey (Antarctic Peninsula), Programma Nazionle di Ricerche in Antartide (Terra Nova Bay), Institut Français pour la Recherche et la Technologie Polaires (Adélie Coast to Dome C), and the Japanese Antarctic Research Expedition (Dome Fuji, Relay Station) supported the AWS program in other areas of Antarctica. The AWS program is supported by the National Science Foundation grant OPP 94-19128.

References

Holmes, R.E., G.A. Weidner, and C.R. Stearns. 1995. Antarctic automatic weather stations: Austral summer 1994–1995. *Antarctic Journal of the U.S.*, 30(5), 327–329.

Holmes, R.E., G.A. Weidner, and C.R. Stearns. 1997. Antarctic automatic weather stations: 1995–1996. *Antarctic Journal of the U.S.*, 32(5).

Nonhydrostatic numerical simulation of antarctic katabatic wind events

THOMAS R. PARISH, LARRY D. OOLMAN, *and* JOHN J. CASSANO, *Department of Atmospheric Science, University of Wyoming, Laramie, Wyoming 82071*

A significant body of antarctic meteorology literature has been dedicated to the persistent, near-surface slope (katabatic) flows (*see* Bromwich and Parish in press and references contained therein). Katabatic winds are forced partly by the radiative cooling of the sloping ice surface (e.g., Parish and Waight 1987; Parish and Wendler 1991) and partly by the large-scale horizontal pressure gradients associated with transient synoptic disturbances (e.g., Parish, Pettré, and Wendler 1993; Yasunari and Kodama 1993).

During the past few decades, significant advances have been made in understanding the meteorology of the lower antarctic atmosphere. Much of the progress can be attributed to the collection of data sets, notably automatic weather stations (AWSs), and subsequent analyses (Bromwich et al. 1993; Wendler et al. 1993). Mathematical simulation of katabatic flows has also been a useful tool in understanding antarctic katabatic winds. Briefly, such modeling involves grid-point solutions of finite difference forms of the hydrodynamical equations governing atmospheric motion. Currently, a number of numerical models exist, and they have been used to simulate the low-level drainage flow regime (Parish 1984; Gallée and Schayes 1992; Hines, Bromwich, and Parish 1995; Seefeldt 1996; Cassano in press). One of the widely used meteorological models is the Pennsylvania State University/National Center for Atmospheric Research Mesoscale Model (MM5). The MM5 equations are written in terrain-following sigma coordinates for use in either a hydrostatic or nonhydrostatic mode. The horizontal and vertical resolution in the model is variable, allowing application to a variety of atmospheric problems. This model has elaborate physics parameterizations to simulate effects such as solar and terrestrial radiation, cloud physics, and turbulence. The model uses standard meteorological data sets for initial conditions and so can be used in a real-time forecast mode.

Assessment of the application of MM5 to the Antarctic is currently underway at the University of Wyoming. This model is being used in both two-dimensional (Cassano in press) and three-dimensional versions. Application of any numerical model to antarctic meteorology presents several challenges.

- A number of physical parameterization schemes exist. Some are better adapted for use in the antarctic environment than others.
- The temperatures and wind fields in the lower antarctic atmosphere meteorology are often strongly influenced by the local topography. As seen with earlier modeling work, it is essential to specify terrain representative for the scale of phenomena of interest. Thus, use of a large-grid spacing [greater than 100 kilometers (km)] such as used in most

operational weather forecast models is inadequate for simulation of local phenomena.

- It is necessary to begin model simulations with appropriate initial conditions for the underlying ice terrain. This requirement often necessitates the use of nonstandard techniques to initialize MM5 and means the user must acquire familiarity with the model.

Figures 1 and 2 illustrate results from one MM5 simulation for Antarctica. The case study in question is from 25 March 1993. During this period, an intense katabatic wind storm damaged wind sensors on AWS units at Port Martin (66.8°S 141.4°E) and Penguin Point (67.2°S 146.0°E; Keller et al. 1995). A nonhydrostatic MM5 simulation was run with an inner and outer domain, each consisting of a 52×52 grid. The grid spacing was set at 60 km for the outer domain and 20 km for the inner domain. The model simulation was for 12 hours commencing at 0000 UTC 25 March 1993. Results at the end of the simulation (1200 UTC) are presented here. Figure 1 illustrates the 12-hour simulated surface pressures (in hectopascals) and streamlines of wind approximately 5 meters above the surface from the outer mesh. An intense cyclone is seen to the north of the continent; streamlines of the airflow suggest a strong control of airflow off the continent by the large-scale horizontal pressure field. The streamline pattern over the continent also suggests high-pressure ridging over the high plateau of East Antarctica. Surface winds appear to display an upslope component across a broad portion of the antarctic continent on the eastern side of the anticyclonic (counterclockwise in the Southern Hemisphere) circulation. Results from the 12-hour simulation for the inner mesh, centered on the Adélie Land terrain, are shown in figure 2. The cyclone and terrain forcing accelerate the surface katabatic winds such that winds in excess of 15 meters per second are seen along the near-coastal margin near 140°E. The simulated winds are weaker than observed, however. AWS units record winds in excess of 30 meters per second at this time. Reasons for this underestimation are currently being investigated.

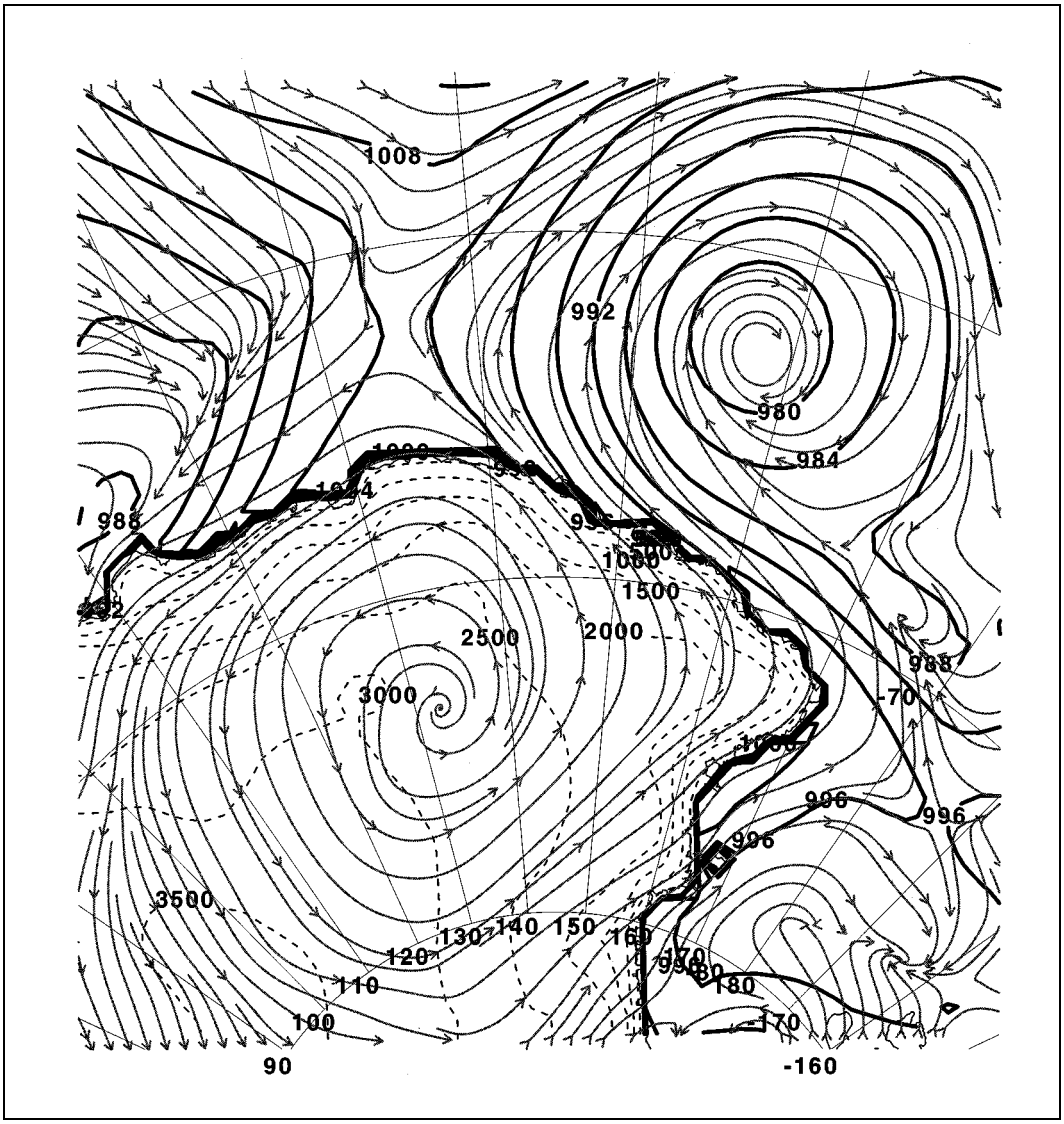

Figure 1. Simulated weather conditions on 1200 UTC 25 March 1993 showing intence cyclone to the north of Antarctica. Surface pressures (in hectopascals) are represented by solid dark lines, streamlines of surface winds in solid, thin lines. Antarctic terrain in dashed lines.

Research is continuing to improve the utility of such modeling efforts. It is hoped that real-time simulations can be routinely provided to enhance forecasting capabilities in the Antarctic. Results of the modeling work will be of use for both research and operational activities.

This research has been supported in part by the National Science Foundation grant OPP 92-18544.

References

Bromwich, D.H., and T.R. Parish. In press. Meteorology of the Antarctic. In D. Karoly and D. Vincent (Eds.), *Meteorology of the Southern Hemisphere*. Boston: American Meteorological Society.

Bromwich, D.H., T.R. Parish, A. Pellegrini, C.R. Stearns, and G.A. Weidner. 1993. Spatial and temporal characteristics of the intense

katabatic winds at Terra Nova Bay, Antarctica. In D.H. Bromwich and C.R. Stearns (Eds.), *Antarctic meteorology and climatology: Studies based on automatic weather stations* (Antarctic Research Series, Vol. 61). Washington, D.C.: American Geophysical Union.

Cassano, J.J. In press. Analysis of east antarctic katabatic winds using two numerical models. (Ph.D. thesis, Department of Atmospheric Science, University of Wyoming, Laramie, Wyoming.)

Gallée, H., and G. Schayes. 1992. Dynamical aspects of katabatic wind evolution in the antarctic coastal zone. *Boundary-Layer Meteorology*, 59, 141–161.

Hines, K.M., D.H. Bromwich, and T.R. Parish. 1995. A mesoscale modeling study of the atmospheric circulation of high southern latitudes. *Monthly Weather Review*, 123, 1146–1165.

Keller, L.M., G.A. Weidner, C.R. Stearns, and M.T. Whittaker. 1995. Antarctic automatic weather station data for the calendar year 1993. Madison, Wisconsin: Department of Atmospheric and Oceanic Sciences, University of Wisconsin.

Parish, T.R. 1984. A numerical study of strong katabatic winds over Antarctica. *Monthly Weather Review*, 112, 545–554.

Parish, T.R., P. Pettré, and G. Wendler. 1993. The influence of large scale forcing on the katabatic wind regime of Adélie Land, Antarctica. *Meteorology and Atmospheric Physics*, 51, 165–176.

Parish, T.R., and K.T. Waight. 1987. The forcing of antarctic katabatic winds. *Monthly Weather Review*, 115, 2214–2226.

Parish, T.R., and G. Wendler. 1991. The katabatic wind regime at Adélie Land. *International Journal of Climatology*, 11, 97–107.

Seefeldt, M.W. 1996. Wind flow in the Ross Island region, Antarctica, based on the UW-NMS with a comparison to automatic weather station data. (M.S. thesis, Department of Atmospheric and Oceanic Sciences, University of Wisconsin, Madison, Wisconsin.)

Wendler, G., J.C. André, P. Pettré, J. Gosink, and T. Parish. 1993. Katabatic winds in Adélie Land. In D.H. Bromwich and C.R. Stearns (Eds.), *Antarctic meteorology and climatology: Studies based on automatic weather stations* (Antarctic Research Series, Vol. 61). Washington, D.C.: American Geophysical Union.

Yasunari, T., and S. Kodama. 1993. Intraseasonal variability of katabatic wind over East Antarctica and planetary flow regime in the Southern Hemisphere. *Journal of Geophysical Research*, 98, 13063–13070.

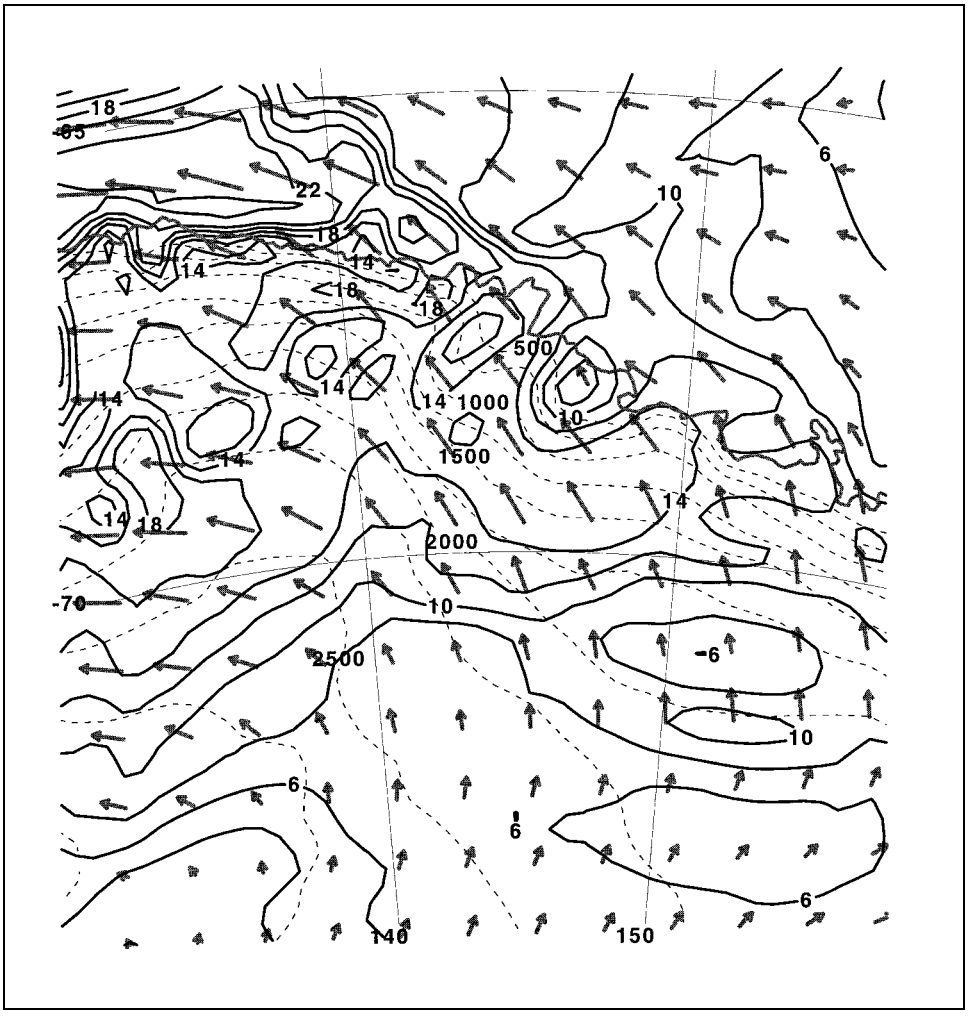

Figure 2. Fine-scale simulation of surface wind conditions on 1200 UTC 25 March 1993. Wind vectors represented by arrows, wind speeds (in meters per second) in solid, dark lines. Antarctic terrain contours in dashed lines.

Ross Island area wind field

CHARLES R. STEARNS, *Space Science and Engineering Center, University of Wisconsin, Madison, Wisconsin 53706*

In the Ross Ice Shelf region of Antarctica, the vertical static stability of the atmosphere is usually stable to the vertical displacement of an air parcel. For example, the annual mean air temperatures for Pegasus North and Minna Bluff automatic weather station (AWS) sites in the figure and given in the table are –21.4°C and –21.7°C, respectively. In the annual mean, the air moving down from the 920-meter (m) height of Minna Bluff to Pegasus North would be 8.9°C warmer than Pegasus North and statically stable to a vertical air parcel displacement. The result is that most of the time the air flow is around, not over, terrain. Stearns and Weidner (1990, 1991, 1993) present additional wind data in the area of the Pegasus Runway.

The figure presents a composite annual vector wind direction and speed for the AWS sites given in the table. The AWS sites, located to the east of Ross Island and Black and White Islands, Laurie, Ferrell, Meeley, Tiffany, and Linda, have similar vector directions out of the south-southwest. The maximum annual wind speed directions are also similar. At Tiffany AWS site, the wind velocity is lower as is the annual mean wind speed. The vector wind direction at Minna Bluff is similar to the previous sites but with a higher velocity. One would expect other sites in the area to have similar vector directions. Manning AWS site, however, clearly shows the effect of the Minna Bluff obstacle on the surface wind as the flow is deflected to the east around Minna Bluff.

The area south and west of Ross Island has a very different flow pattern. As the air moves from Tiffany AWS site toward Windless Bight where Katie AWS site is located, it is deflected by the 200 m plus barrier formed by Mount Erebus, Mount Terra Nova, Mount Terror, and Hut Point Peninsula to flow from the northeast along Hut Point Peninsula toward Black Island and Brown Peninsula. The warmer air above 200 m flows over the Hut Point Peninsula to the west based on the records from Fogle AWS site on Hut Point Peninsula. AWS sites south of Brown Peninsula also show air flowing to the west. Slotten and Stearns (1987) reported that the pressure difference between Katie AWS site and the AWS sites of Laurie, Ferrell, and Meeley increased with increasing wind speed at Katie AWS site.

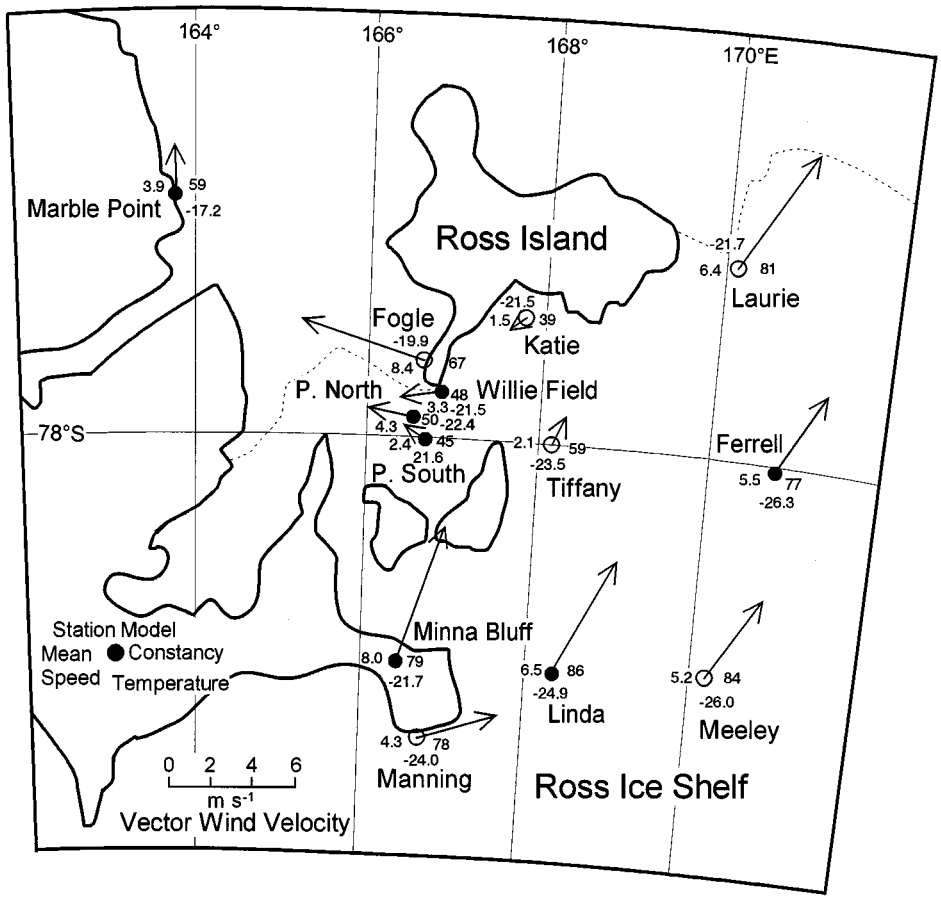

Map of the Ross Island, Antarctica, area with a composite of the vector wind direction and velocity in the area showing the effect of the obstacles on the wind flow. The actual data used are given in the table along with the year or months of the year that were used for the figure. The differences between years at one site are small compared to the differences between the AWS sites.

The table shows that the highest wind speeds at all AWS sites are from 175° to 246°. These are wind events in which the stability changes from stable to neutral or slightly unstable allowing the strong winds coming over Minna Bluff to reach the surface at Pegasus North and South possibly influencing the operation of aircraft from Pegasus Runway. When strong winds are present at the surface, the change of wind speed with

Data from AWS sites

NOTE: The differences between the wind data for different years at the same site are small compared to the differences between the sites.

Site name	Elevation (in meters)	1[a]	2	3	4	5	6	7	8	9
Meeley	49	212	4.4	5.2	84	224	24	–26.0	1982	
Ferrell	45	207	4.2	5.5	77	211	27	–26.3	1982	
Fogle	202	109	6.0	8.9	67	175	34	–19.9	1984	FMAMJJASON
Katie	40	52	0.6	1.5	39	188	19	–21.5	1985	
Laurie	23	213	5.2	6.4	81	234	36	–21.7	1985	FMAMJND
Manning	66	255	3.8	4.3	78	246	23	–24.0	1985	
Tiffany	25	201	1.2	2.1	59	195	28	–23.5	1985	
Marble Point	120	179	2.3	3.9	59	237	30	–17.2	1986	
Pegasus North	10	101	2.0	4.3	50	195	34	–21.4	1994	
Pegasus South	10	125	1.0	2.4	45	206	20	-21.6	1994	
Willie Field	40	86	1.5	6.5	48	210	24	–22.4	1994	
Linda	50	206	5.6	6.5	86	210	31	–24.9	1995	JFMAMJD
Minna Bluff	920	199	6.3	8.0	79	198	46	–21.7	1995	

[a]1 = resultant wind direction; 2 = vector wind velocity for the year in meters per second (m s^{-1}); 3 = mean scalar wind speed for the year in m s^{-1}; 4 = ratio of the vector wind velocity to the scalar wind speed times 100; 5 = direction of the maximum wind speed for the year in m s^{-1}; 6 = magnitude of the maximum wind speed for the year in m s^{-1}; 7 = mean air temperature for the year in °C; 8 = year of the record; 9 = months that the data were collected if the AWS unit did not function throughout the year.

height is sufficient to introduce a possible wind shear effect on aircraft turning to a northerly course after takeoff from either Pegasus Runway or Williams Field.

This research is supported by the National Science Foundation grant OPP 94-19128.

References

Slotten, H.R., and C.R. Stearns. 1987. Observations of the dynamics and kinematics of the atmospheric surface layer on the Ross Ice Shelf, Antarctica. *Journal of Climate and Applied Meteorology*, 26, 1731–1743.

Stearns, C.R., and G. Weidner. 1990. Wind speed events and wind direction at Pegasus site during 1989. *Antarctic Journal of the U.S.*, 25(5), 258–262.

Stearns, C.R., and G. Weidner. 1991. Wind speed, wind direction, and air temperature at Pegasus North during 1990. *Antarctic Journal of the U.S.*, 26(5), 251–253.

Stearns, C.R., and G. Weidner. 1993. Snow temperature, wind speed, and wind direction around the Pegasus Runway during 1992. *Antarctic Journal of the U.S.*, 28(5), 291–294.

On the reflectivity and radiation budget of antarctic sea ice

G. WENDLER*, B. MOORE, D. DISSING, *and* J. KELLEY, *University of Alaska–Fairbanks, Fairbanks, Alaska 99775*

*Present address: *International Centre for Antarctic Information and Research, Christchurch, New Zealand*

During the course of the year, the areal extent of antarctic sea ice varies a great deal. The normal maximum amount in late winter is 19×10^6 square kilometers; the minimum in late summer is only 3.5×10^6 square kilometers. The presence or absence of sea ice influences strongly the energy transfer between ocean and atmosphere and is of great importance in understanding climate (Radok, Streten, and Weller 1975). In the coastal region, the interaction of the sea ice with the semi-permanent katabatic winds is of special importance (Wendler, Gilmore, and Curtis 1997).

Most of the studies on the radiative characteristics of sea ice have been carried out in the Arctic (e.g., Hansen 1961). Ice conditions around Antarctica, however, are not similar to those in the Arctic, a fact known for a long time. In March 1840, Charles Wilkes wrote in a letter to Sir James Clark Ross: "The ice of the Antarctic is of totally different character from that of the Arctic." (cited from Kearns and Britton 1955). The majority of the sea ice around Antarctica melts in summer, so that unlike the Arctic, where a large amount of multiyear ice is present, most ice encountered is first-year ice and thin (mostly <1 meter). Comparable radiative studies of sea ice using a ship as a platform were carried out by Allison, Brandt, and Warren (1993) and Wendler et al. (1997).

In 1997, we analyzed the reflectivity and the radiation budget of sea ice, data obtained from the 1995–1996 USCGC Polar Star cruise, which went from Hobart, Tasmania, to McMurdo, Antarctica, to open up the sound for tanker and other support ship traffic. During this cruise, radiative and meteoro-

logical measurements were carried out continuously. Short-wave incoming and reflected radiation, ultraviolet radiation, long-wave incoming and outgoing fluxes as well as numerous meteorological and support data were obtained. Some of the results follow.

The incoming solar radiation had a mean value of 217 watts per square meter ($W m^{-2}$); this was a relatively weak value due to the large amount of fractional cloud cover observed. For a large part of the trip, the Sun was above the horizon for 24 hours a day. Looking at the mean diurnal variation, a maximum of 461 $W m^{-2}$ was observed around local noon, whereas the minimum was 40 $W m^{-2}$ at midnight. Daily courses for individual days varied widely, depending mostly on the amount and type of clouds and to a lesser degree on the position of the ship and atmospheric turbidity. A maximum mean daily global value of 305 $W m^{-2}$ was observed on 10 January 1996, a partly cloudy day; the minimum (139 $W m^{-2}$) was observed on 25 December 1995, a day with a thick layer of stratus overcast and occasional snowfall.

The albedo varied widely and was found to be a function not only of ice concentration but also of ice type. If the sea ice was snow covered, especially high values were observed. Two-minute values for an hour close to solar noon are presented in figure 1. For calm sea conditions (figure 1*A*) values around 6 percent were found for water; they increased with both decreasing solar elevations and sea stage. On 22 December 1995, a very stormy day with wind speeds in excess of 20 meters per second and a large amount of white caps, values up to 23 percent were observed (figure 1*B*). In figure 1*C*, the transition from 10/10 sea ice to open-water conditions is depicted. Although the albedo of the snow-covered sea ice was 67 percent, it dropped to 18 percent in less than an hour, indicating a relatively well-pronounced ice edge, which was observed on 26 December 1996. Ice conditions, however, can be much more variable as can be seen in figure 1*D*. Albedo values between 11 and 69 percent were observed during this hour, indicating a large variation in ice concentration over a relatively small area. Although the albedo is fairly constant for each ice type, it varies considerably from type to type. For thin ice (figure 1*E*), the values varied little during the hour. A mean value of 34 percent was observed with a maximum deviation of 2 percent. Such low values are in agreement with Kukla and Robinson (1980). Flooded sea ice (figure 1*F*), which we observed on 27 December 1995, showed similar values to thin ice (figure 1*E*); however a much larger variation in albedo than with the thin ice was observed. The values varied between 22 and 43 percent. In contrast to broken ice, which showed a similar or larger magnitude in the total value, the variation in space is much smoother for flooded ice. Finally, snow-covered pack ice (figure 1*G*) showed high, fairly constant values. For an hour on 13 January 1996, a mean value of 74 percent was observed.

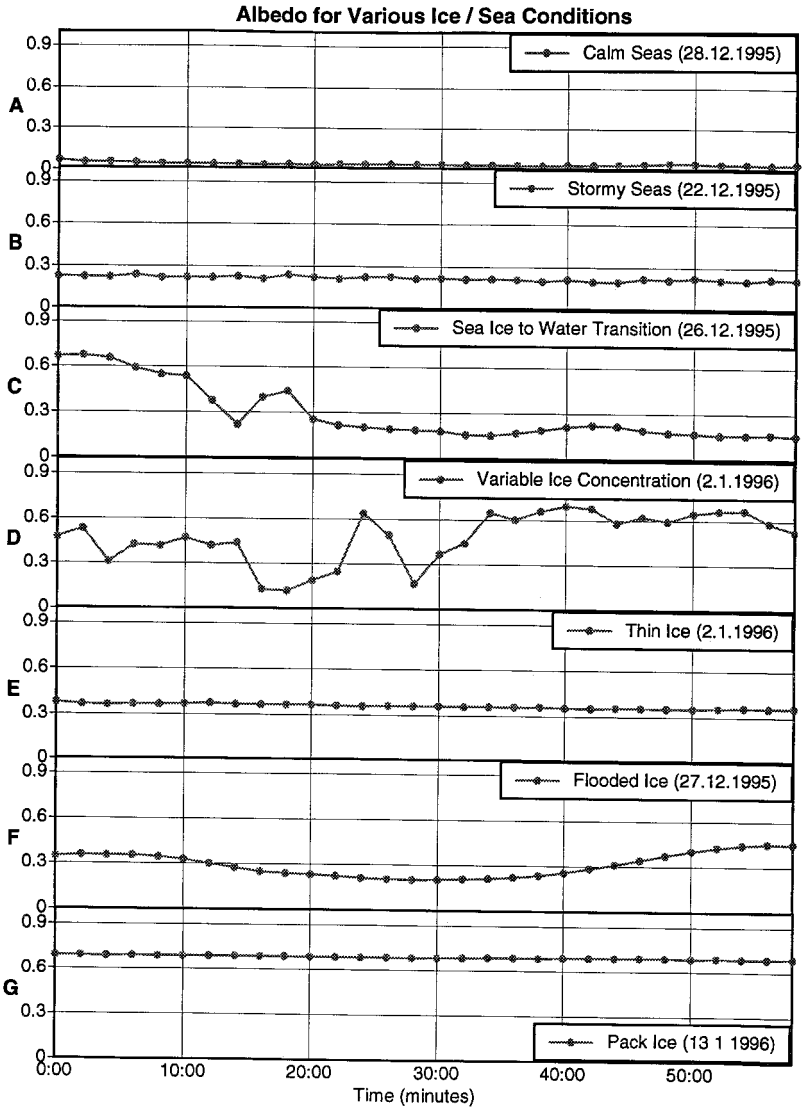

Figure 1. Albedo observations (2-minute values) for different surfaces over the southern oceans.

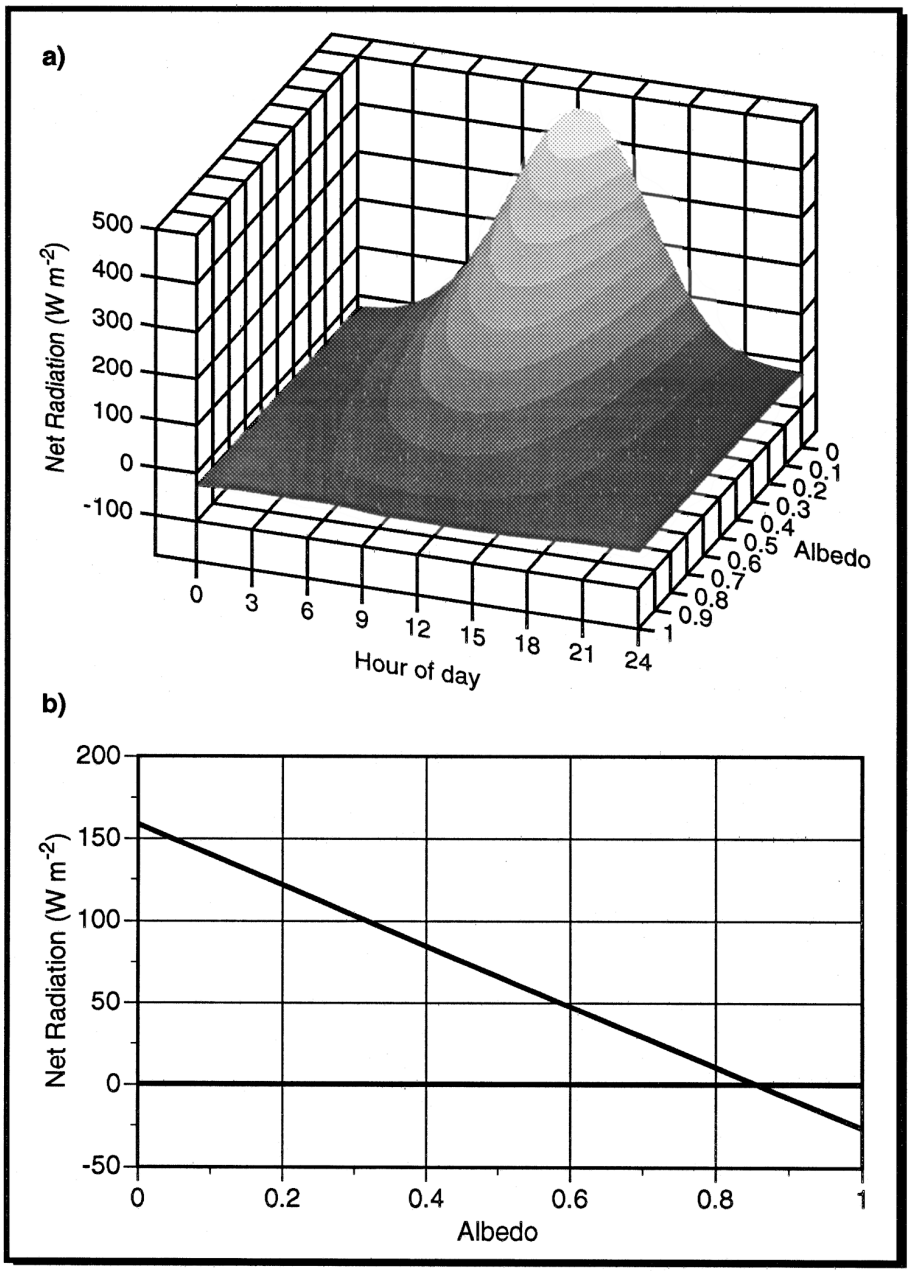

Figure 2. Diurnal variation (*A*) and mean daily values (*B*) of modeled net radiation as function of surface albedo. The observed global radiation and the net long-wave radiation were used as input into the model.

Typical values of the outgoing long-wave radiation vary between 250 W m^{-2} and 300 W m^{-2}. Outgoing radiation tended to decrease with increasing ice concentration, which is, of course, an effect of the cooler surface temperature.

The long-wave incoming radiation is mostly a function of cloudiness and, to a lesser degree, dependent on the water vapor content and turbidity of the atmosphere. These values do not show a systematic diurnal variation for our cruise. The values are normally smaller than the outgoing long-wave radiation, resulting in mean negative net long-wave radiation values. The mean value, –27 W m^{-2}, represents only about 10 percent of the outgoing flux. In other words, about 90 percent of the long-wave outgoing surface radiation is radiated back from the clouds and the atmosphere. This value is high and a result of the large amount of the fractional cloud cover. The net long-wave radiation shows the smallest losses during the early morning hours (–23 W m^{-2}), when the surface temperature is at a minimum, and the greatest losses in the early afternoon (–33 W m^{-2}), when the surface temperature has its maximum.

For the observed albedo and long-wave radiation values, modeling results show (figure 2) that the net radiation was always positive when averaged over a day. The magnitude and diurnal variation, however, depended strongly on the surface albedo. Integrating over a day (figure 2*B*), one sees that an albedo in excess of 85 percent is necessary to obtain a negative balance. During our trip, mean hourly albedo values were seen to range from 6 percent to about 70 percent, an indication that the net radiation was positive. This result is the expected one because the ice around Antarctica melts during the summer months.

Although the albedo, and with it the short-wave radiation budget, is strongly influenced by the presence of sea ice, the long-wave radiation budget is affected to a much lesser degree. The outgoing radiation is a function of the surface temperature; hence, the infrared losses from an ice-covered surface are always equal to or less than those for sea water. There is only a very small diurnal variation of about 10 W m^{-2} following roughly the diurnal course of the air temperature.

This research was supported by National Science Foundation grant OPP 94-13879. We thank the captain and crew of the

Polar Star as well as the helicopter detachment, which supported us wonderfully. Science Officer Matt Smith, who helped us a great deal, deserves special mention. C. Stearns and J. Cassano from the University of Wisconsin serviced/installed the automatic weather station. A. Hauser read and improved this manuscript. To all of them our sincere thanks.

References

Allison, I., B. Brandt, and S. Warren. 1993. East antarctic sea ice: Albedo, thickness distribution, and snow cover. *Journal of Geophysical Research,* 98, 12417–12429.

Hansen, K.J. 1961. Albedo of sea ice and ice islands in the Arctic Ocean basin. *Arctic,* 14(3), 188–196.

Kearns, W., and B. Britton. 1955. *The silent continent.* New York: Hauper and Brothers Publication.

Kukla, G., and P. Robinson. 1980. Annual cycle of surface albedo. *Monthly Weather Review,* 108(1), 56–68.

Radok, U., N. Streten, and G. Weller. 1975. Atmosphere and ice. *Oceanus,* 18(4), 15–27.

Wendler, G., U. Adolphs, A. Hauser, and B. Moore. 1997. On the surface energy budget of sea ice. *Journal of Glaciology,* 43(143), 122–130.

Wendler, G., D. Gilmore, and J. Curtis. 1997. On the formation of coastal polynyas in the area of Commonwealth Bay, Eastern Antarctica. *Atmospheric Research,* 664(1), 55–76.

Solar radiation processes in the east antarctic sea-ice zone

STEPHEN G. WARREN, *Department of Atmospheric Sciences, University of Washington, Seattle, Washington 98195*
COLLIN S. ROESLER, *Department of Marine Science, University of Connecticut, Groton, Connecticut 06340*
RICHARD E. BRANDT, *Department of Atmospheric Sciences, University of Washington, Seattle, Washington 98195*

Seasonal sea ice covers a large part of the Southern Hemisphere and plays an important role in the climate of the southern oceans. The input of solar energy to the ocean is limited by reflection from the snow/ice system and absorption within the ice. The goals of this study are to investigate

- the reflection of solar radiation by the variety of snow and sea-ice types in the Antarctic and
- the concentrations, distributions, and absorption properties of organic material in the snow and sea ice to evaluate its role in the absorption of solar radiation, trapping of heat, and the summertime decay of the ice.

The experiment is a follow-on to work begun on the first topic in 1988 (Allison, Brandt, and Warren 1993). The project was expanded in 1996 to cover other types of ice not sampled in the 1988 experiment, as well as to make measurements with a greater spectral range and to initiate a study of absorptive constituents (Roesler and Iturriaga 1994).

Fieldwork was carried out in collaboration with the Australian Antarctic Division on voyage 2 of the *Aurora Australis*, by all three authors, during the springtime period 26 September to 25 November 1996 during which all types of new and young ice could be sampled, as well as first-year ice. Similar studies of melting snow and ice are planned for November and December 1999 in the marginal ice zone.

In addition, studies of green icebergs consisting of frozen seawater were possible on this voyage, extending the studies begun in the 1988 experiment (Warren et al. 1993).

Optical measurements and ice sampling from the ship's basket

A spectral radiometer, covering the wavelength range 320 to 1,060 nanometers (nm) with 11 filters, and a pyranometer were used to measure the incident and reflected irradiance for the determination of cloud transmission and ice albedo. They were mounted on the end of a 3-meter (m) carbon-fiber tube supported on the inboard end by an aluminum frame. The frame could be mounted either in a basket to be hung from the ship's crane or in a helicopter with a sliding window. This apparatus was designed to position the radiometers as far as possible horizontally from the basket, so that the ice being sampled would be minimally shadowed by the basket. The frame allowed positioning, leveling, and inverting of the radiometers. A second radiometer, covering the wavelength range 410 to 683 nm with seven filters, each of 10-nm bandwidth, was used to measure incident and transmitted irradiance through the ice. This instrument was deployed through the ice on an articulating arm, which positioned the instrument on the underside of the ice 0.5 m from the hole.

Most measurements were made within 2 hours of solar noon to maximize the solar altitude. The basket was hung off the sunny side of the ship to avoid shadowing of the ice by the ship. The surface types sampled were water, grease ice, pancakes, nilas, snow-covered nilas, and snow-covered first-year ice (FYI). Spectral albedos are shown in figure 1. Visible transmission varied from more than 90 percent for grease ice to 40 percent for pancakes. Samples of all ice types were collected for analysis of organic constituents.

Measurements on first-year floes and fast ice

Vertical profiles of snow density and grain size were measured at several ice-floe stations and at the fast ice at Davis Station (68°S 79°E). These are the principal variables affecting transmission and reflection of sunlight by snow. Spectral albedos were obtained for FYI with a variety of snow thicknesses. Particularly valuable was a site on 1.5-m-thick fast ice because it included a scene of naturally snow-free and nearly snow-free sea ice (near the coast, where strong winds

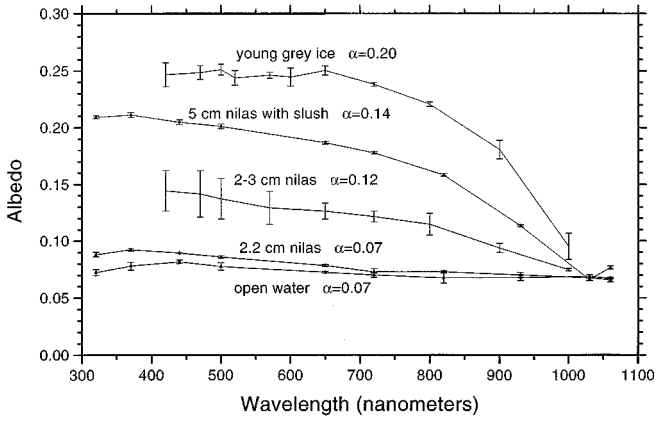

Figure 1. Spectral albedo of new and young ice types. The two samples with restricted spectral range were measured in 1988; the other three in 1996. Allwave albedos (α) are also given.

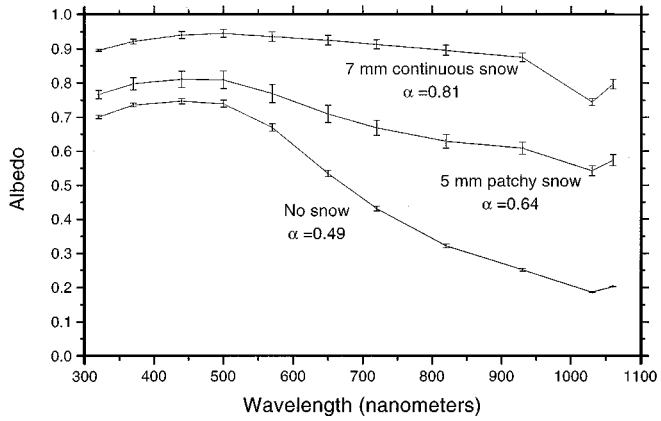

Figure 2. Spectral albedo of 1.8-meter-thick sea ice near Davis Station (68°S 79°E), covered with 0, 5, or 7 millimeters of snow.

often blow the snow away). The large enhancement of albedo due to very thin snow layers of 5 and 7 millimeters is illustrated in figure 2.

Hundred-meter transects were established on the floes ranging from uniform thin gray ice (0.25 m) to highly ridged annual ice (>6 m). Spectral transmission at visible wavelengths, snow thickness, and ice thickness were measured at 10-m spacings along the 100-m transects. Where time permitted, ultraviolet transmission in four wavebands was also measured. Snow samples and ice cores were collected from the 0-m, 50-m, and 100-m stations. Temperatures were measured at the snow/ice and air/snow interfaces. Ice temperatures were measured at 5-centimeter intervals along the ice cores immediately after retrieval.

Visible transmission decreased from 20 percent for ice thickness of 0.25 m to less than 1 percent for 1 m; however, the variations in attenuation per meter of ice were strongly dependent upon the relative concentrations of frazil, granular, and columnar ice in the ice column. Spectral variations associated with algae and entrapped organic material were observed in the transmission spectra; they will be quantified by optical analyses of the ice samples.

Icebergs

In our earlier work, we discussed the origin and composition of green icebergs calved from the Amery Ice Shelf and sampled near Mawson Station (Warren et al. 1993). To evaluate the generality of those conclusions, two green icebergs (probably calved from the West Ice Shelf) were sampled near Davis Station. Albedos are shown in figure 3 for a large iceberg containing sections of bubbly blue ice, clear blue ice, clear green ice, and cloudy yellow-green ice. The spectral peak moves from 450 to 575 nm in the progression from blue to yellow-green ice. Oxygen isotope analyses show that the bubbly blue ice is glacial ice; the other three types are marine ice consisting of desalinated frozen seawater. The organic constituents responsible for the variations in color will be analyzed. The blue marine ice is likely to contain far less dissolved

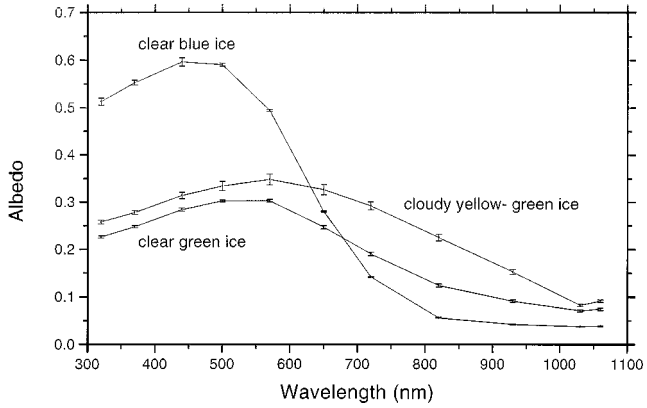

Figure 3. Spectral albedo of three parts of a composite iceberg, all consisting of "marine ice" (formed by freezing of seawater, probably to the base of an ice shelf).

organic matter than the green or yellow-green ice or than the green iceberg we sampled in 1988.

Ice-sample analyses

Ice cores and snow samples were returned to the freezer container on the ship for processing. Ice cores were sectioned into 5-cm-long samples. The samples from cores, thin ice, and icebergs are now undergoing analysis at the University of Connecticut for salinity, algal pigment concentration, particle identification and size distribution, particulate and dissolved spectral absorption coefficients, and, as necessary, thin sections.

Downward solar spectral irradiance

In an attempt to determine cloud radiative forcing in the antarctic sea-ice zone, we measured the spectral and total irradiance transmitted through clouds, as well as the irradiance from clear skies. Taking surface albedo into account, cloud optical thickness will be inferred.

Acknowledgments

We thank Ian Allison for sponsoring our collaboration with the Australian Antarctic Division and the Antarctic Cooperative Research Centre, Kelvin Michael and Martin Betts for coordination of experiments on voyage 2, Don Perovich for the loan of an ultraviolet radiometer, and Vin Morgan for oxygen isotope analyses. This research was supported by National Science Foundation grants OPP 95-27244 and OPP 95-27245.

References

Allison, I., R.E. Brandt, and S.G. Warren. 1993. East antarctic sea ice: Albedo, thickness distribution, and snow cover. *Journal of Geophysical Research*, 98, 12417–12429.

Roesler, C.S., and R. Iturriaga. 1994. Absorption properties of marine-derived particulate and dissolved material in Arctic sea ice. *SPIE Ocean Optics XII*, 2258, 933–943.

Warren, S.G., C.S. Roesler, V. Morgan, R.E. Brandt, I. Goodwin, and I. Allison. 1993. Green icebergs formed by freezing of organic-rich seawater to the base of antarctic ice shelves. *Journal of Geophysical Research*, 98, 6921–6928 & 18309.

Chlorine-containing gases in Antarctica

M.A.K. KHALIL, *Department of Physics, Portland State University, Portland, Oregon 97207*
R.A. RASMUSSEN, *Department of Environmental Science and Engineering, Oregon Graduate Institute, Portland, Oregon 97291*

In recent years, there has been considerable interest in chlorine-containing trace gases in the atmosphere, particularly in Antarctica because of the relationship between chlorofluorocarbons and the antarctic ozone hole. All chlorine-containing trace gases, whether produced by human activities or by natural processes, have a potential for destroying ozone in the stratosphere. This is a complex environmental problem, but it is clear that manmade chlorine-containing gases are the driving force behind the antarctic ozone hole and, by extension, reductions of stratospheric ozone over other parts of the world [World Meteorological Organization (WMO) 1989, 1991, 1995].

We have taken measurements of the major chlorine-containing gases in Antarctica for more than 20 years, first at Amundsen–Scott South Pole Station and more recently at Palmer Station (64.46°S 64.04°W). Here we report the results of this work. During recent years, major changes in the concentration of ozone-depleting compounds have taken place in Antarctica because of the Montreal Protocol, which is designed to phase out the production of chlorofluorocarbons and related compounds, to prevent the destruction of the ozone layer (WMO 1995).

The production and emissions of chlorofluorocarbons have been declining in recent years [Alternative Fluorocarbon Environmental Acceptability Study (AFEAS) 1997]. These changes are quite dramatic, and in the last year or so, the production of the major chlorofluorocarbons has fallen to between 10–20 percent of the peak values in the 1980s; emissions have fallen accordingly. These changes in industrial emissions are clearly observable in the antarctic atmosphere. The concentrations of many chlorine-containing compounds are either increasing very slowly compared to previous years or are decreasing. Consequently, for the first time in the 20 years of observations, the total chlorine concentrations in Antarctica have declined from one year to the next during the last 2 years. The trends we discuss for Antarctica are also representative of the global changes, although the magnitudes may be different at other latitudes.

Trends of chlorinated compounds in Antarctica

Chlorinated compounds can be classified as "reactive" or "unreactive." Reactive gases are taken to be those that are removed in the troposphere (approximately surface to 12 kilometers). Gases that are not removed in the troposphere have the greatest potential for destroying the ozone layer. Such gases are classified as unreactive.

"Reactive chlorine" gases are the following: methylchloroform (CH_3CCl_3) and chlorodifluoromethane ($CHClF_2$, F-22), which are entirely manmade, and methylcloride (CH_3Cl), which is thought to be mostly natural, but substantial amounts are known to be emitted from biomass burning. Small amounts of "other chlorine-containing gases" are also expected to exist in the antarctic atmosphere, namely trichloroethylene (C_2HCl_3), tetrachloroethylene (C_2Cl_4), chloroform ($CHCl_3$), dichloroethane ($C_2H_4Cl_2$), dichloromethane (CH_2Cl_2), and bromochloromethane (CH_2BrCl), because these have been measured at latitudes down to about 45°S. Many of these gases have some natural emissions, mostly from the oceans. All known natural emissions of chlorine-containing gases are from this group (Khalil in press).

"Unreactive" gases in the troposphere are dichlorofluoromethane (CCl_2F_2, F-12), trichlorofluoromethane (CCl_3F, F-11), carbon tetrachloride (CCl_4), and the fully halogenated ethanes ($C_2Cl_3F_3$, F-113; $C_2Cl_2F_4$, F-114; C_2ClF_5, F-115).

Figure 1*A* shows the chlorine composition for the antarctic atmosphere. It is determined as the concentration times

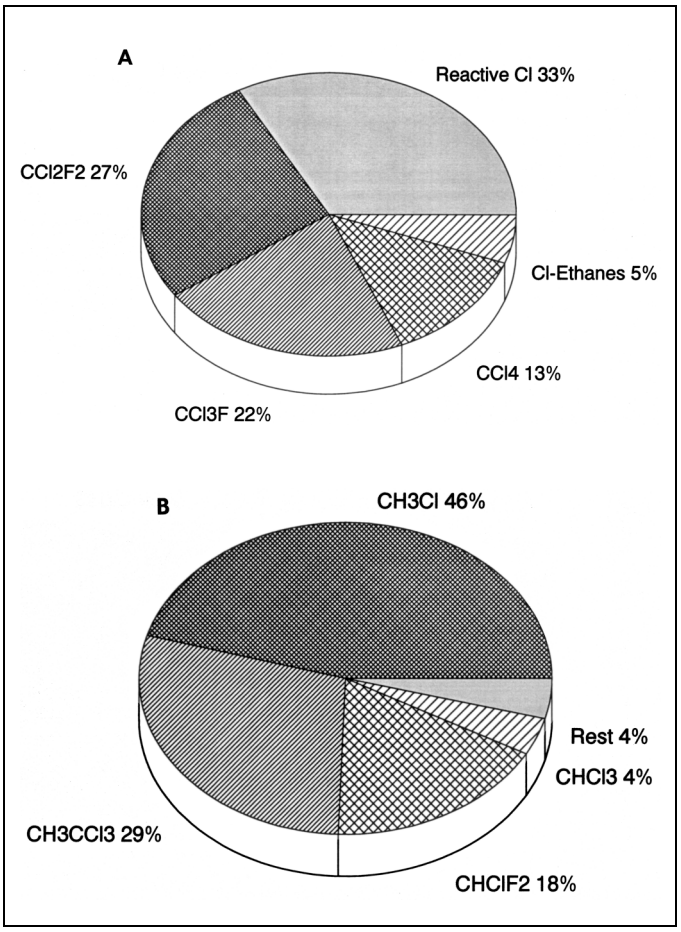

Figure 1. *A*. The distribution of chlorine in the gas phase in Antarctica. About two-thirds is from the manmade chlorofluorocarbons and at least half of the "reactive chlorine" group are also from human activities. The graph shows the concentration as the percent of chlorine contributed by each gas to the total chlorine composition of the antarctic atmosphere (see text). *B*. The reactive chlorine gases in the antarctic atmosphere. All known natural emissions of chlorine-containing gases are from this group.

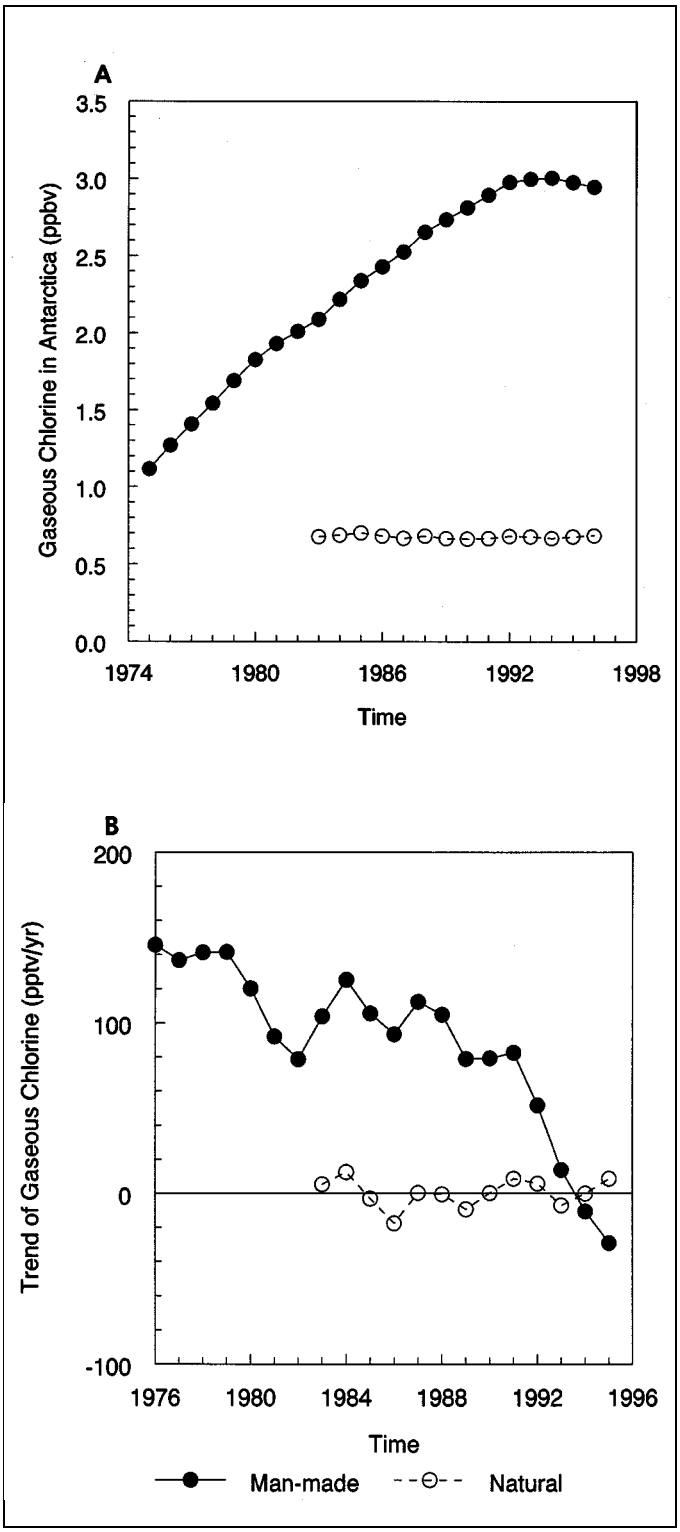

Figure 2. *A*. The 20-year record of total gaseous chlorine in Antarctica. Concentrations are in parts per billion (ppbv) chlorine. *B*. The rate of change (trend) of chlorine containing gases in parts per trillion per year (pptv/yr). During the last 2 years, the concentration of total chlorine has begun to drop in Antarctica.

the number of chlorine atoms in the molecule of the gas. The "reactive chlorine" component is further expanded in figure 1*B*. It is not clear as to how much gaseous chlorine comes from natural processes. There are, however, no documented natural sources of the unreactive compounds, and from the reactive chlorine group, there are no known natural sources of methylchloroform and chlorodifluoromethane, so at least 80–85 percent of the chlorine present in the antarctic atmosphere is of anthropogenic origins. The remainder is mostly methylchloride and chloroform, and there is about 50 parts per trillion by volume (pptv) of the "other chlorine-containing gases" mentioned above. We are designating these as "natural," although it is not proven to be so, and some may be manmade.The record of annually averaged concentrations of chlorine in the antarctic atmosphere is shown in figure 2*A* representing 20 years of observational data. It is determined as the sum of the concentrations of each gas times the number of chlorine atoms in each molecule of the gas and given in parts per billion. In figure 2*B*, we show the trends at year t, where trend $(t)=[C(t+1)+C(t-1)]/2$ in parts per trillion per year. Sources of data are Rasmussen and Khalil (1986), Khalil and Rasmussen (1992), and continuation of these experiments and Montzka et

al. (1996) for $CHClF_2$. For F-113 and F-22, there are no measurements before 1986 and 1992, respectively. For the calculations here, concentrations were estimated by linear backward extrapolation based on the earliest 4 years of data. Concentrations of both these gases were small during the early periods and, thus, do not greatly affect the total chlorine shown here.

The results show a pattern that is being observed worldwide. Because most of the gases involved are produced in the middle northern latitudes, these changes are delayed at Antarctica by 1–2 years. Concentrations of methylchloroform (CH_3CCl_3), which has been used as a de-greasing solvent, are declining rapidly because it has a relatively short lifetime of about 6 years. Carbon tetrachloride, which was used for the production of fluorocarbons, is declining because these compounds are no longer being produced. The trend of F-11, one of the major chlorofluorocarbons implicated in the depletion of the ozone layer, is also beginning to decline. F-113 is no longer increasing in the atmosphere. Only chlorofluorocarbon-12 continues to increase, but the trend is much less than in previous years.

Conclusions

New chemicals are now being used instead of the chlorofluorocarbons we have discussed here. The main new compounds are HCFC-141b ($C_2H_3Cl_2F$), HCFC-142b ($C_2H_3ClF_2$), and HCFC 134a ($C_2H_2F_4$). These and $CHClF_2$ (F-22) are taking over the usages of chlorofluorocarbons in air conditioning, refrigeration, and blowing insulating foams and as solvents. These gases belong to the group of "reactive chlorine." Most of the emissions will be removed in the troposphere and will never reach the stratosphere where they may affect the ozone layer.

Acknowledgments

Portions of this work were supported by grants from the National Science Foundation (OPP 87-17023 and GEO 96-96080) and the Department of Energy (DE-FG06-84ER60313). Support for the data analysis was provided by the Chemical Manufacturer's Association through the Chlorine Chemical Council and from the European Chemical Industry Council (CEFIC) through Euro Chlor. Additional support was provided by the Andarz Co.

References

Alternative Fluorocarbon Environmental Acceptability Study (AFEAS). 1997. *Production, sales and atmospheric release of fluorocarbons through 1995*. AFEAS, Science and Policy Services, Inc., West Tower—Suite 400, 1333 H Street N.W., Washington, DC 20005.

Khalil, M.A.K. In press. Reactive chlorine compounds in the atmosphere. In P. Fabian (Ed.), *Handbook of environmental chemistry*. Heidelberg: Springer-Verlag.

Khalil, M.A.K., and R.A. Rasmussen. 1992. Trace gases over Antarctica: Bromine, chlorine and organic compounds involved in global change, *Antarctic Journal of the U.S.*, 27(5), 267–269.

Montzka, S.A., J.H. Bulter, R.C. Meyers, T.M. Thompson, T.H. Swanson, S.D. Clark, L.T. Lock, and J.W. Elkins. 1996. Decline in the tropospheric abundance of halogen from halocarbons: Implications for stratospheric ozone depletion. *Science*, 272, 1318–1322.

Rasmussen, R.A., and M.A.K. Khalil. 1986. Atmospheric trace gases: Trends and distributions over the last decade. *Science*, 232, 1623–1624.

World Meteorological Organization (WMO). 1989. *Scientific assessment of ozone depletion* (Global Ozone Research and Monitoring Project, report no. 20). Geneva, Switzerland: WMO.

World Meteorological Organization (WMO). 1991. *Scientific assessment of ozone depletion* (Global Ozone Research and Monitoring Project, report no. 25). Geneva, Switzerland: WMO.

World Meteorological Organization (WMO). 1995. *Scientific assessment of ozone depletion* (Global Ozone Research and Monitoring Project, report no. 37). Geneva, Switzerland: WMO.

Lidar observations of stratospheric aerosol and temperatures at McMurdo Station during 1996

GUIDO DI DONFRANCESCO, *Ente per le Nuove Tecnologie, L'Energia E L'Ambiente Casaccia, Dipartimento Ambiente 00060, Rome, Italy*

ALBERTO ADRIANI *and* FRANCESCO CAIRO, *Istituto Fisica dell'Atmosfera, Consiglio Nazionale delle Ricerche, Rome, Italy*

Since 1993, an optical radar or lidar (light detection and ranging) has been operating at McMurdo Station (78°S 167°E) during winter and spring. The instrument, described in more detail by Adriani et al. (1992), uses a pulsed laser source with 150 millijoules per pulse at 532 nanometers. The system can monitor the presence of volcanic aerosol and clouds in the atmosphere above the station by measuring the light backscattered from the atmosphere. In fact, after system calibration, the received signal is compared with the one expected from an atmosphere not containing particles. In this way, a parameter called backscattering ratio *R* is calculated. When particles are not present, *R* gives the value of 1, and any value larger than 1 is related to the presence of particles [usually between 5 and 25 kilometers (km) altitude]. Detectable particles in the antarctic stratosphere are due to large volcanic eruptions (e.g., Mount Pinatubo, June 1991) and to polar stratospheric clouds (PSCs). The latter form during the polar winter when the temperature drops below 195–196 K, and playing an important role in the heterogeneous chemistry of the polar stratosphere, they are strictly linked with formation of the "ozone hole." The kind of particles found in a PSC depends on the local temperature at the time of the observation as well as on the previous thermal history of the air mass in which the cloud has formed (Gobbi and Adriani 1993; Adriani et al. 1995).

The emitted laser light is polarized, and the lidar is able to detect the depolarization of the backscattered light induced by PSCs (the depolarization value *D* can be defined as the ratio between the depolarized and polarized lidar backscattering). In fact, spherical particles, as liquid droplets, do not depolarize the backscattered light, whereas aspherical particles do induce depolarization. So it is possible to discern among different kinds of particles (crystalline, amorphous, liquid) from the state of polarization of the backscattered light.

Figure 1 shows *R* (backscattering ratio) and *D* (depolarization) versus altitude and time. The first 2 months (Julian days between 90 and 150) show the background volcanic aerosol. PSC formation (steeply increasing *R* values) is observed in the period from June to September. Some of these clouds show a presence of ice particles (high values of depolarization), depending not only on the temperature at the time of the observation but also on the temperatures previously experienced by the observed air masses. Such ice clouds are observed in particular between mid-July and mid-August when the stratospheric temperature reaches the lowest values. On those occasions, *R* values up to 20 and *D* values up to 50 percent are measured above 20 km.

Above 25 km, the received signal is proportional to the molecular density of

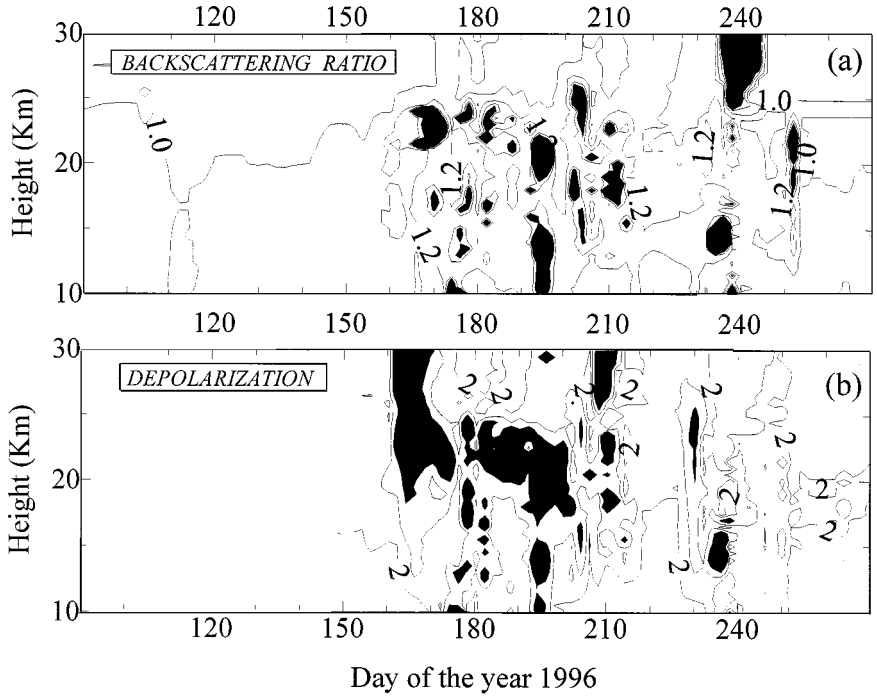

Figure 1. Backscattering ratio (*A*) and depolarization (*B*) versus julian day and altitude in the 1996 above McMurdo Station. Black area denotes values higher than 1.5 (*A*) and 5 (*B*).

the air, and it is possible to retrieve by lidar the temperature profiles as described by Hauchecorne and Chanin (1980). Using our system, which averages the profiles (performed every 3–4 days) along the daily period of measurement (0.5 hour) and filters vertically to approximately 6 km of altitude resolution, we obtain temperature profiles between 25 and 65 km of altitude with an average temperature statistical error of 0.2 K at 25 km, 1.5 K at 40 km, and 10 K at 55 km.

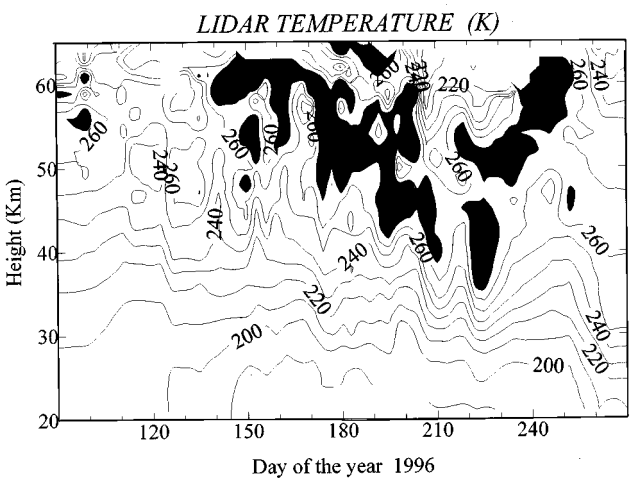

Figure 2. As figure 1 but for the lidar temperatures. Black area denotes values higher than 270K.

Currently, satellite and lidar remote sensing are considered the most suitable methods for observing middle atmosphere temperatures. Satellites offer better coverage but lower accuracy and vertical resolution with respect to remote sensing, which is, however, localized and can perform only nocturnal observations. In wintertime, however, temperature retrievals by satellites may be unreliable under highly disturbed conditions such as stratospheric warmings (Di Donfrancesco et al. 1996).

Figure 2 shows temperature behavior versus altitude and time (day of the year) as measured by the lidar above McMurdo Station between 1 April and 1 October 1996. The stratosphere was very active during June and August, and strong perturbations (stratospheric warmings) appeared in the region between 40 km and 60 km altitude.

This work has been supported by Programma Nazionale Ricerche in Antartide. We would like to thank National Science Foundation and Antarctic Support Associates from the United States of America for giving us the opportunity to operate the lidar at McMurdo Station in wintertime. Thanks are due to F. Cardillo for his software assistance.

References

Adriani, A., T. Deshler, G. Di Donfrancesco, and G.P. Gobbi. 1995. Polar stratospheric clouds and volcanic aerosol during the 1992 spring McMurdo, Antarctica: Lidar and particle counter comparative measurements. *Journal of Geophysical Research*. 100(12), 25877–25897.

Adriani, A., T. Deshler, G.P. Gobbi, B.J. Johnson, and G. Di Donfrancesco. 1992. Polar stratospheric clouds over McMurdo, Antarctica, during the 1991 spring: Lidar and particle counter measurements. *Geophysical Research Letters* 19(17), 1755–1758.

Di Donfrancesco, G., A. Adriani, G.P. Gobbi, and F. Congeduti. 1996. Lidar observations of stratospheric temperature above McMurdo Station, Antarctica. *Journal of Atmospheric and Terrestrial Physics*, 58(13), 1391–1399.

Gobbi, G.P., and A. Adriani. 1993. Mechanisms of formation of stratospheric clouds observed during the antarctic late winter of 1992. *Geophysical Research Letters*, 20(14), 1427–1430.

Hauchecorne, A., and M.L. Chanin. 1980. Density and temperature profiles obtained by lidar between 35 and 70 km. *Geophysical Research Letters*, 7, 565–568.